Tili E, Michaille JJ, Cimino A, Costinean S, Dumitru CD, Adair B, Fabbri M, Alder H, Liu CG, Calin GA and Croce CM (2007) Modulation of miR-155 and miR-125b levels following lipopolysaccharide/TNF-α stimulation and their possible roles in regulating the response to endotoxin shock. *J Immunol* **179:** 5082-5089.lack endogenous FGF-2. *Mol Cancer Res* **2:** 653-661.

Volinia S, Calin GA, Liu CG, Ambs S, Cimmino A, Petrocca F, Visone R, Iorio M, Roldo C, Ferracin M, Prueitt RL, Yanaihara N, Lanza G, Scarpa A, Vecchione A, Negrini M, Harris CC and Croce CM (2007) A microRNA expression signature of human solid tumors defines cancer gene targets. *Proc Natl Acad Sci U S A* **103:** 2257-2261

Zeng Y, Wagner EJ and Cullen BR (2002) Both natural and designed micro RNAs can inhibit the expression of cognate mRNAs when expressed in human cells. *Mol Cell* **9:** 1327-1333.

Zhu S, Si ML, Wu H and Mo YY (2007) MicroRNA-21 targets the tumor suppressor gene tropomyosin 1 (TPM1). *J Biol Chem* **282:** 14328-14336.

II. 研究成果の刊行に関する一覧表

別紙４
研究成果の刊行に関する一覧表
雑誌

発表者氏名	論文タイトル名	発表誌名	巻号	ページ	出版年
Rawiwan Maniratanachote, Keichi Minami, Miki Katoh, Miki Nakajima and Tsuyoshi Yokoi	Chaperone proteins involved in troglitazone-induced toxicity in human hepatoma cells.	Toxicological Sciences	83	293-302	2005
Yusuke Hara, Miki Nakajima, Ken-Ichi Miyamoto, and Tsuyoshi Yokoi	Inhibitory effects of psychotropic drugs on mexiletine metabolism in human liver microsomes: predictionof in vivio drug interactions.	Xenobiotica	35	549-560	2005
Keiichi Minami, Toshiro Saito, Masatoshi Narahara, Hiroyuki Tomita, Hirokazu Kato, Miki Katoh, Miki Nakajima and Tsuyoshi Yokoi	Relationship between hepatic gene expressionprofiles and hepatotoxicity in five typical hepatotoxicant-administered rats .	Toxicological Sciences	87	296-305	2005
Miki Nakajima, Yuto Fujiki, Satoru Kyo, Taro Kanaya, Mitsuhiro Nakamura, Yoshiko Maida, Masaaki Tanaka, Masaki Inoue, and Tsuyoshi Yokoi	Pharmacokinetics of paclitaxel in ovarian cancer patients and genetic polymorphisms of *CYP2C8*, *CYP3A4*, and *MDR1*.	Journal of Clinical Pharmacology	45	674-682	2005
Rawiwan Maniratanachote, Ayaka Shibata, Shuichi Kaneko, Takanobu Wakasugi, Takeshi Sawazaki, Kanefusa Katoh, Shogo Tokudome, Miki Nakajima, and Tsuyoshi Yokoi	Identivication of autoantibody to aldolase B in sera from patients with troglitazone-induced liver disfunction. liver disfunction.	Toxicology	216	15-23	2005

Hiroyuki Yamanaka, Miki Nakajima, Yusuke Hara, Miki Katoh, Osamu Tachibana, Junkoh Yamashita, and Tsuyoshi Yokoi	Urinary excretion of phenytoin metabolites, 5-(4'-hydroxyphenyl)-5-phenylhydantoin and its *O*-glucuronide in humans and analysis of genetic polymorphisms of UDP-glucuronosyltransferases.	Drug Metabolism and Pharmacokinetics	20	135-143	2005
Hiroyuki Yamanaka, Miki Nakajima, Tatsuki Fukami, Haruko Sakai, Akiko Nakamura, Miki Katoh, Masataka Takamiya, Yasuhiro Aoki, and Tsuyoshi Yokoi	CYP2A6 and CYP2B6 are involved in nornicotine formation from nicotine in humans: Interindividual differences in these contributions.	Drug Metabolism and Disposition	33	1811-1818	2005
Keiichi Minami, Rawiwan Maniratanachote, Miki Katoh, Miki Nakajima, and Tsuyoshi Yokoi	Simultaneous measurement of gene expression for hepatotoxicity in thioacetamide-administered rats by DNA macroarrays.	Mutation Research	603	64-73	2006
Yuki Tsuchiya, Miki Nakajima, Shingo Takagi, Miki Katoh, Wenchao Zheng, Colin R Jefcoate, and Tsuyoshi Yokoi.	Binding of steroidogenic factor-1 to the regulatory region might not be critical for transcriptional regulation of human *CYP1B1* gene.	Journal of Biochemisty	139	527-534	2006
Miki Katoh, Naoto Suzuyama, Toshiyuki Takeuchi, Sumie Yoshitomi, Satoru Asahi, and Tsuyoshi Yokoi.	Kinetic analyses for species differences in P-glycoprotein-mediated drug transport.	Journal of Pharmaceutical Science	95	2673-2683	2006
Rawiwan Maniratanachote, Miki Katoh, Miki Nakajima, and Tsuyoshi Yokoi.	Dephosphorylation of ribosomal protein P0 in response to troglitazone-induced cytotoxicity.	Toxicological Letters	166	189-199	2006

Yuki Tsuchiya, Miki Nakajima, Shingo Takagi, Takao Taniya, and Tsuyoshi Yokoi.	MicroRNA regulates the expression of human cytochrome P450 1B1.	Cancer Research	66	9090-9098	2006
Naoto Suzuyama, Miki Katoh, Toshiyuki Takeuchi, Sumie Yoshitomi, Tomoaki Higuchi, Satoru Asashi, and Tsuyoshi Yokoi.	Species differences of inhibitory effects on P-glycoprotein-mediated drug transport.	Journal of Pharmaceutical Science	96	1609-1618	2007
Miki Nakajima, Hiroyuki Yamanaka, Ryoichi Fujiwara, Miki Katoh, and Tsuyoshi Yokoi.	Stereoselective glucuronidation of 5-(4'-hydroxyphenyl)-5-phenyl hydantoin by human UDP-glucuronosyltransferase (UGT) 1A1, UGT1A9, and UGT2B15: effects of UGT-UGT interactions.	Drug Metabolism and Disposition	35	1679-1686	2007
Miki Katoh, Tomohito Matsui, and Tsuyoshi Yokoi.	Glucuronidation of antiallergic drug, tranilast: identification of human UDP-glucuronosyltransferase isoforms and effect of its phase I metabolite.	Drug Metabolism and Disposition	35	583-589	2007
Sho Akai, Hiroko Hosomi, Keiichi Minami, Koichi Tsuneyama, Miki Katoh, Miki Nakajima, and Tsuyoshi Yokoi	Knock down of g-glutamylcysteine synthetase in rat causes acetaminophen-induced hepatotoxicity.	Journal of Biological Chemistry	282	23996-24003	2007
Tatsuki Fukami, Miki Nakajima, Haruko Sakai, Miki Katoh, and Tsuyoshi Yokoi	CYP2A13 metabolizes the substrates of human CYP1A2, phenacetin, and theophylline.	Drug Metabolism andDisposition	35	33-339	2007
Yusuke Hara, Miki Nakajima, Ken-ichi Miyamoto, and Tsuyoshi Yokoi	Morphine glucuronosyltransferase activity in human liver microsomes is inhibited by a variety of drugs that are co-administered with morphine.	Drug Metabolism and Pharmacokinetics	22	103-112	2007

Hirotoshi Okumura, Miki Katoh, Keiichi Minami, Miki Nakajima, and Tsuyoshi Yokoi	Change of drug excretory pathway by CCl4-induced liver dysfunction in rat.	Biochemical Phrmacology	74	488-495	2007
Hiroyuki Yamanaka, Miki Nakajima, Miki Katoh, and Tsuyoshi Yokoi	Glucuronidation of thyroxine in human liver, jejunum, and kidney microsomes.	Drug Metabolism and Disposition	35	1679-1686	2007
Shinichi Takagi, Miki Nakajima, Takuya Mohri, and Tsuyoshi Yokoi	Post-transcriptional regulation of human pregnane X receptor by microRNA affects the expression of cytochrome P450 3A4.	Journal of Biolgical Chemistry		in press	
Rawiwan Maniratanachote and Tsuyoshi Yokoi	A mechanistic view of troglitazone hepatotoxicity	Hepatotoxicity: From Genomics to in vitro and in vivo. John Wiley & Sons, Ltd.		299-311	2007

TOXICOLOGICAL SCIENCES 83, 293–302 (2005)
doi:10.1093/toxsci/kfi022
Advance Access publication November 3, 2004

Chaperone Proteins Involved in Troglitazone-Induced Toxicity in Human Hepatoma Cell Lines

Rawiwan Maniratanachote, Keiichi Minami, Miki Katoh, Miki Nakajima, and Tsuyoshi Yokoi[1]

Drug Metabolism and Toxicology, Division of Pharmaceutical Sciences, Graduate School of Medical Science, Kanazawa University, Kakuma-machi, Kanazawa 920-1192, Japan

Received August 3, 2004; accepted October 25, 2004

Troglitazone (TRO), an effective thiazolidinedione antidiabetic agent, was reported to produce idiosyncratic hepatotoxic effects in some individuals. In contrast, rosiglitazone (RSG), in the same group of agents, has no significant toxic effects and now is widely used. In this study, human hepatoma (HepG2) cell lines were exposed to various doses of TRO as well as RSG (0, 25, 50, and 75 μM) for 48 h. Cell lysates were separated by two-dimensional electrophoresis, and the gels were stained with coomassie brilliant blue to compare the spot profiles. The greatest protein expression at a MW of 75 kDa and isoelectric point of 5 was specifically increased with TRO treatments of 50 and 75 μM. The spot was identified as a mixture of immunoglobulin heavy chain binding protein (BiP) and, to a lesser extent, protein disulfide isomerase-related protein (PDIrp). Immunoblot analyses showed that the BiP protein was dose-dependently increased by TRO treatment and, to a lower degree, by RSG. These effects were also correlated with the high induction of BiP mRNA by TRO (50 and 75 μM) and the lower induction by RSG. However, both treatments showed no significant effects on PDIrp expression. The toxic effects of TRO in relation to the overexpression of BiP were also demonstrated in HLE cells, another human hepatoma cell line. In HLE cells, the inhibition of BiP expression by small interference RNA rendered cells more susceptible to the toxic effects of TRO. These results suggest that the overexpression of BiP is a defense mechanism of the endoplasmic reticulum in response to TRO-induced toxicity.

Key Words: **troglitazone; BiP; chaperone protein; hepatotoxicity; thiazolidinedione.**

Troglitazone (TRO) is one of the thiazolidinedione (TZD) oral antidiabetic agents launched in 1997. This drug has been demonstrated to improve hyperglycemia, hyperinsulinemia, and hypertriglyceridemia, as well as to ameliorate the insulin sensitivity of the target tissues (Fujiwara *et al.*, 1988; Nolan *et al.*, 1994). Based on its pharmacological advantages and the apparent absence of severe toxic effects, TRO was thought likely to become a promising treatment for type II diabetes mellitus in patients with insulin resistance. However, in the early clinical trials, 1.9% of the patients who received TRO experienced an elevation of serum alanine aminotransferase of more than three times the normal upper limit (Watkins and Whitcomb, 1998). During the following few years of utilization, TRO has been reported to produce idiosyncratic hepatotoxic effects in some individuals (Gitlin *et al.*, 1998; Neuschwander-Tetri *et al.*, 1998; Shibuya *et al.*, 1998). Because of the seriousness of the cases, TRO was considered for withdrawal from the market in 2000. The mechanism by which TRO induced toxicity is still not completely understood. Severe hepatotoxic effects have not been observed in any kind of conventional animal models including monkey, which has a similar metabolic profile to human (Rothwell *et al.*, 2002; Watanabe *et al.*, 1999).

The antidiabetic effects of TZDs occur via the activation of peroxisome proliferator-activated receptor γ (PPARγ), and the potency correlates to their receptor-binding activities (Lehmann *et al.*, 1995). There is a less clear association between hepatotoxicity and rosiglitazone (RSG), another TZD agent (Freid *et al.*, 2000; Isley and Oki, 2000; Lebovitz *et al.*, 2002). Since hepatotoxicity is unique to TRO, it is unlikely to be related to a PPARγ class effect.

Even though TRO toxicity has not been observed in *in vivo* experimental animal studies, a number of *in vitro* experiments revealed evidence that TRO can cause apoptotic cell death in various hepatic cell types (Bae and Song, 2003; Tirmenstein *et al.*, 2002; Yamamoto *et al.*, 2001). The degree of lethality also depends on the concentration of the agent and the duration of exposure. Tirmenstein *et al.* (2002) reported that TRO induces mitochondria permeability transition and decreases in the cellular ATP concentration prior to cell death. Regarding the signaling pathway of apoptosis, Bae and Song (2003) reported that TRO but not RSG activates both c-Jun N-terminal protein kinase (JNK) and p38 kinase and causes an increase in proapoptotic proteins such as Bad and Bax, release of cytochrome c, and cleavage of Bid, together with a decrease in antiapoptotic protein, Bcl-2.

In addition to the known mechanisms of apoptotic cell death caused by TRO, we attempted to investigate the involvement of proteins whose up- or down-regulation correlated with the TRO-induced toxic effects. Using a proteomic analysis strategy, we analyzed a protein spot on a gel separated by two-dimensional

[1] To whom correspondence should be addressed. Fax: +81-76-234-4407, E-mail: TYOKOI@kenroku.kanazawa-u.ac.jp.

electrophoresis (2-DE) at an approximate MW of 75 kDa and isoelectric point of 5 that increased greatly in correlation with the concentration-dependent exposure to TRO. The spot was identified as a mixture of two chaperones, immunoglobulin heavy chain binding protein (BiP or Grp78) and, to a lesser extent, protein disulfide isomerase-related protein (PDIrp or ERp72). These findings suggest that TRO targets the endoplasmic reticulum (ER) and causes the overexpression of BiP, a prominent chaperone, in response to cytotoxicity. A possible association of BiP in TRO-induced cytotoxicity is also discussed.

MATERIALS AND METHODS

Cell culture condition and treated agents. Human hepatoma cell lines HepG2 and HLE were obtained from the Riken Gene Bank (Tsukuba, Japan, http://www.rtc.riken.go.jp) and the Japanese Collection of Research Biosources (Tokyo, Japan, http://cellbank.nihs.go.jp/cellbank_e.html), respectively. The cells were maintained in Dulbecco's Modified Eagle's Medium (DMEM, Nissui Pharmaceutical, Tokyo, Japan) containing 10% fetal bovine serum (FBS, BioWhitaker, Walkersville, MD), 3% glutamine, and 8% sodium bicarbonate at 37°C in a humidified atmosphere with 5% CO_2. TRO and RSG were kindly provided by Sankyo (Tokyo, Japan). The treated agents were dissolved in dimethyl sulfoxide (DMSO, Wako, Osaka, Japan), in which the final concentration did not exceed 0.1%. In all treatment conditions, the cells were grown in medium containing 5% FBS.

Cytotoxicity assay. To assess the cytotoxicity, a crystal violet assay and an ATP-based luminescent assay were used. Crystal violet assay was used according to Nakagawa *et al.* (1996) for determining the concentration- and time-dependent toxicity in HepG2 cells. Briefly, a suspension of HepG2 cells (1×10^5 cells/well) in the presence of TZDs or 0.1 % DMSO was seeded onto 12-well plates. At the end of treatment, adherent cells were washed three times with phosphate buffered saline (PBS), fixed with 3.7% formaldehyde, and stained with 0.2% crystal violet. The absorbance at 620 nm was measured after extracting the cells with 2% sodium dodecyl sulfate (SDS). Percent cell viabilities were calculated by comparing them to the absorbance of 0.1% DMSO-treated cells.

Cell viabilities based on the quantity of the ATP produced by metabolically active cells were assessed with a CellTiter-Glo Luminescent assay kit (Promega, Madison, WI) according to the manufacturer's protocol. In the concentration-dependent study, a suspension of HepG2 cells (3×10^3cells/well) in the presence of TZDs or 0.1 % DMSO was seeded onto a 96-well plate. At the end of treatment, CellTiter-Glo reagent was added at an equal volume to the cell culture medium present in each well. The generated luminescent signal was monitored on a Wallac 1420 multilabel counter (PerkinElmer, Wellesley, MA).

Preparing cell lysates. HepG2 cells were treated with various doses of TRO or RSG. At the end of the 48-h treatment period, the cells were harvested by treatment with 0.05% trypsin plus 0.02% EDTA. The cells were washed with PBS and lysed with 100–200 µl of lysis solution (8 M urea, 4% CHAPS, 2% Pharmalyte 3-10) containing protease inhibitors (1 mM DTT, 0.5 mM APMSF, 2 µg/ml aprotinin, 2 µg/ml pepstatin, and 2 µg/ml leupeptin). The cell suspension was centrifuged at 12,000 rpm for 1 h to remove cell debris. The supernatant was collected, and the protein concentration was measured using a Bio-Rad Protein Assay Kit (Bio-Rad Laboratories, Hercules, CA). The cell lysates were stored at −80°C until the time of analysis.

2-Dimensional electrophoresis (2-DE). The devices and chemicals used in 2-DE were purchased from Amersham Biosciences, Buckinghamshire, UK. For the first dimension, 500 µg of protein of the cell lysates was mixed with Destreak Rehydration Solution containing immobilized pH gradient (IPG) buffer of pH 4–7 and applied onto IPG gel strips. The samples were rehydrated at 20°C for 14 h and subsequently separated at 17,500 V-h using an Ettan IPGphor Isoelectric Focusing System. The second dimensional electrophoresis was run on 10% acrylamide gel at 10°C for 4 h. The separated proteins on 2-DE were visualized by coomassie brilliant blue (CBB) staining.

Protein identification. The amino acid sequence analyses from the CBB-stained two-dimensional (2-D) gels were performed at Hitachi Science Systems, Ltd., Japan. The protein spot of interest was excised from the CBB-stained gel of the sample treatment with 75 µM TRO. After in-gel digestion with trypsin, the peptides were reduced and carbamidomethylated. The peptide mass mapping was performed on an ESI-TRAP and analyzed by LC/MS/MS. The matched peptides were searched using MASCOT (http://www.matrixscience.co.uk) based on the NCBInr database.

Western blot analysis. The HepG2 cell lysates (50 µg for BiP, and 25 µg proteins for PDIrp and PDI proteins) were separated on 10% SDS–polyacrylamide gels and transferred onto PVDF membrane (Immobilon-P, Millipore, Billerica, MA). The specific proteins were detected by mouse anti-KDEL monoclonal antibody (SPA-827, Stressgen, San Diego, CA) for BiP, rabbit anti-ERp72 polyclonal antibody (SPA-720, Stressgen) for PDIrp, and rabbit anti-PDI polyclonal antibody (SPA-890, Stressgen) for PDI proteins at dilutions of 1:200, 1:2000, and 1:2000, respectively. The protein bands were developed by biotinylated second antibody-peroxidase reaction. The quantitative analysis of protein expression was performed using a densitometer GS-700 (Bio-Rad Laboratories).

Reverse transcription and real-time PCR. Human hepatoma cells were treated with or without TZDs. At the end of the incubation periods, the cells were washed with PBS, and the total RNA was prepared using Isogen® (Nippon Gene, Tokyo, Japan) according to the manufacturer's instructions. Reverse transcription (RT) reactions were carried out by incubating 2 µg of total RNA with random primer (Takara, Tokyo, Japan) and Moloney-Murine Leukemia Virus Reverse transcriptase (M-MLV-RT) RNaseH Minus (Toyobo, Tokyo, Japan) at 37°C for 1 h. Subsequently, the steady state of the mRNA levels was quantified by fluorescence-based real-time PCR. Oligonucleotide sense and antisense primers of human-BiP (5′-TGCTTGATGTATGTCCCCTTA-3′ and 5′-CCTTGTCTTCAGCTGTCACT-3′) and PDIrp (5′-AATACCAGGATGCCGCTAAC-3′ and 5′-GCAAAGGTGTACTCAGGGAA-3′) as well as GAPDH (5′-CCAGGGCTGCTTTTAACTC-3′ and 5′-GCTCCCCCCTGCAAATGA-3′) were used. The reaction mixture for real-time PCR containing 1 µl of RT product, Ex Taq R-PCR Version (Takara, Japan), SYBR® Green I (Molecular Probes, Eugene, OR), and the specific sense and antisense primers were subjected to a Smart Cycler® System (Cepheid, Sunnyvale, CA). After a holding step at 95°C for 30 s, the thermal cycling was repeated for 45 cycles of 94°C for 4 s and 64°C for 20 s, followed by melting from 60°C to 95°C at 0.2°C/s. The standard curve for the relative quantification was created by serially diluted GAPDH concentrations plotted against the threshold cycle number from the real-time PCR reaction. The BiP and PDIrp expressions were evaluated, and the relative values were normalized with the GAPDH values from the same DNA samples.

siRNA generation. Small interference RNA (siRNA) for BiP (Accession AF188611) and human lamin A (Accession X03444) mRNA target sequences were created and checked by the species-appropriate genome database (http://www.ncbi.nlm.nih.gov/BLAST/) to avoid target sequences homologous to other known coding sequences. The sense and antisense primers for BiP were 5′-CAACTGTTACAATCAAGGTC-3′ and 5′-CTGTATCCTCTTCACCAGTT-3′, and for lamin A were 5′-AAAGCGCGCAATACCAAGAA-3′ and 5′-CCTCACTGTAGATGTTCTTC-3′, designed with the T7 RNA polymerase promoter sequences (CTAATACGACTCACTATAGGGAGG) at the 5′-end of each primer. The target genes were amplified by PCR and purified by ethanol precipitation. dsRNAs were generated using a T7 RiboMAX™ Express Large Scale RNA Production System Kit (Promega) according to the manufacturer's protocol. The dsRNAs were then diced into 20–23 bp of siRNAs by incubating them with recombinant dicer enzyme (GTS, San Diego, CA) for 18 h. The obtained siRNAs were further subjected to two purification steps, removal of the salts with a Sephadex G25 column (Amersham Biosciences) and the undigested dsRNA by centrifugation with a Microcon YM-100 (Millipore). The purified siRNA duplexes were stored at −80°C until analysis.

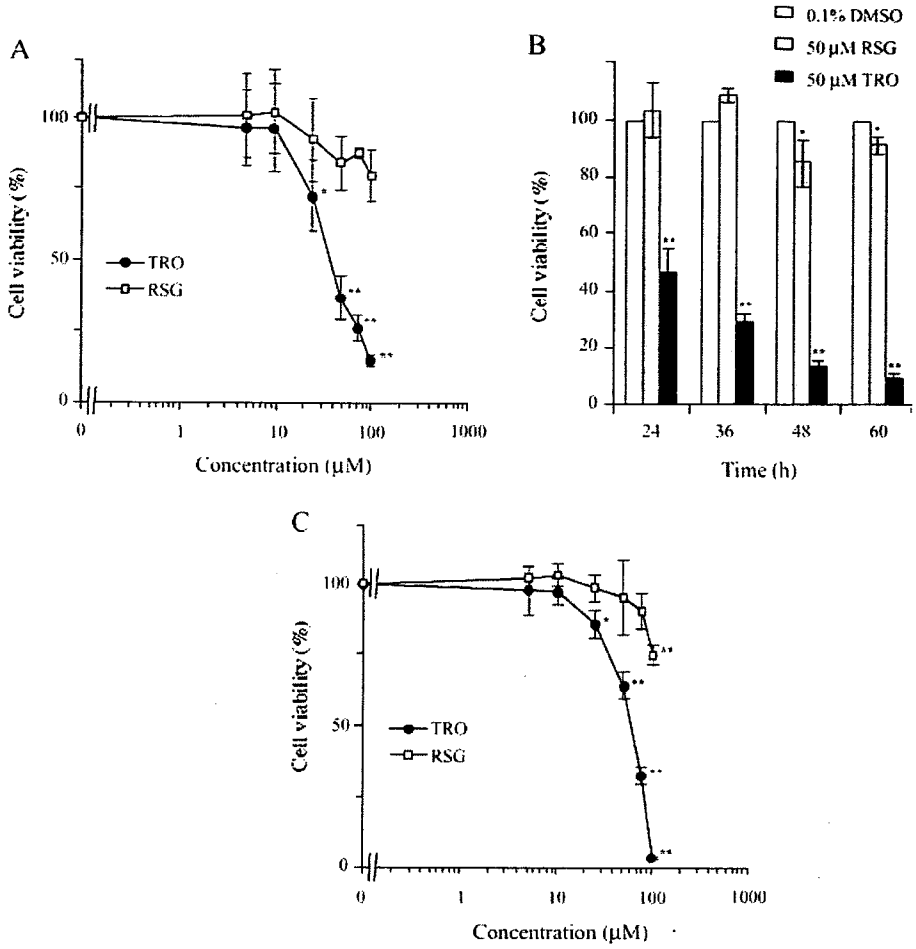

FIG. 1. TZDs cytotoxicity in HepG2 cells. (A) HepG2 cells were incubated with 0.1% DMSO (control) or the indicated concentration of TRO or RSG for 48 h. (B) HepG2 cells were incubated with 0.1% DMSO (control) or 50 μM TZDs for the indicated time. Cell viabilities were assessed by crystal violet assay. (C) HepG2 cells were incubated with 0.1% DMSO (control) or the indicated concentration of TRO or RSG for 48 h. Cell viabilities were measured by ATP-based luminescent assay. The results represent the mean ± SD of at least three independent experiments. $*p < 0.05$, $**p < 0.01$ compared with the control.

Transfection of siRNA. In order to knockdown target genes at the transcriptional level, siRNA was transfected into the cells. Because of the difficulty to transfect siRNA into HepG2 cells, HLE cells, another human hepatoma cell line that demonstrates similar BiP expression profiles to HepG2 cells (data not shown), were used in this experiment. Briefly, HLE cells were seeded onto 6-well plates (8×10^4 cells/well) or 96-well plates (3×10^3 cells/well) and incubated for 24 h before transfection. At approximately 30–50% confluency, the cells were transfected with siRNA using Oligofectamine (Invitrogen, Carlsbad, CA) for 24 h. The cells were treated with TZDs or DMSO at the concentrations indicated for 24 h before analysis.

Statistical analysis. Data were analyzed by one-way analysis of variance (ANOVA) followed by Dunnett's post hoc test using Instat version 2.0 software; $p < 0.05$ was considered significant.

RESULTS

Troglitazone-Induced HepG2 Cell Toxicity

To investigate the toxic effects of TRO, crystal violet assay was used to determine the concentration- and time-dependent cytotoxicity. ATP-based luminescent assay was used for the sensitive detection of a small amount of viable cells. In the concentration-dependent experiment, HepG2 cells were exposed to various concentrations of TRO of 0 (0.1% DMSO), 5, 10, 25, 50, 75, and 100 μM as well as the same concentrations of RSG as negative controls. After 48 h of treatment, ≥25 μM TRO significantly reduced the cell viability with an approximate IC_{50} of 40 μM, whereas RSG showed no significant toxic effects (Fig. 1A). TRO also showed a time-dependent cytotoxicity in HepG2 cells from 24 h to 60 h of exposure ($p < 0.01$) compared to the DMSO treatment (Fig. 1B). The concentration-dependent cytotoxicity of TRO (Fig. 1A) was comparable to the reduction of ATP produced by viable metabolically active cells as detected by the ATP-based luminescent assay (Fig. 1C).

Proteomic Analysis for Troglitazone-Induced Hepatotoxicity

The different toxic effects of TRO and RSG were investigated by proteomic analysis to determine the differences in the protein

expression profiles. HepG2 cells were treated with or without various doses of TRO or RSG for 48 h. Cell lysates were prepared and subjected to 2-DE analysis. The gels were then stained with CBB. A number of spots were up- and down-regulated by the treatments. We focused on the spot showing a large amount of protein expression, which showed dose-dependent and TRO-specific changes, at an approximate MW of 75 kDa and isoelectric point of 5. The expression was increased by treatment with 50 and 75 μM of TRO (Fig. 2A). At the same position, RSG-treated cells demonstrated no difference compared to the DMSO-treated control (Fig. 2B). The spot was excised, subjected to amino acid sequence analysis and identified as a mixture of immunoglobulin binding protein (BiP) (Fig. 3A) and, to a lesser extent, protein disulfide isomerase-related protein (PDIrp or ERp72) (Fig. 3B). Notably, BiP was prominent in this finding, as indicated by the higher total score (1341) compared to PDIrp (294), and these proteins had MWs and calculated isoelectric point values near the position that appeared on the 2-D gels.

Changes of Chaperone Proteins and mRNAs by TZDs Exposure

HepG2 cells were incubated in the presence of various concentrations of TRO or RSG or 0.1% DMSO (control) for 48 h. The cell lysates were confirmed for the expressions of BiP and PDIrp proteins by Western blot analyses with specific antibodies. In Figure 4A, BiP protein detected by anti-KDEL antibody was markedly increased in intensity by increasing the TRO concentration and was about 5-fold at 100 μM. The same phenomenon was also demonstrated with RSG treatment but with a relatively smaller increase, even at 100 μM (about 2.5-fold). The expression of PDIrp as detected by anti-ERp72 antibody showed no significant difference among the treatments (Fig. 4B). We also investigated the expression of PDI protein and there was no significant difference (Fig. 4C). To further investigate the control of BiP and PDIrp expressions at the transcription level, the mRNAs were determined by real-time PCR. Comparing the results from the Western blot analyses, BiP mRNA expression by TRO treatment was also dose-dependently induced, with the highest level at 75 μM (about 11-fold) (Fig. 5A). However, at 100 μM of TRO, BiP mRNA was comparable to the control because of cell toxicity. RSG-treated cells showed a small tendency to increase, with significance at the higher doses of 75 and 100 μM (Fig. 5A). Although PDIrp protein was equally expressed in the presence of all treatments, mRNA expression in response to TRO and RSG treatment showed the induction at the doses of 75 and 100 μM (Fig. 5B).

Inhibition of BiP Expression by siRNA

All the above results demonstrated the obvious effects of TRO compared to RSG on BiP overexpression. To clarify these

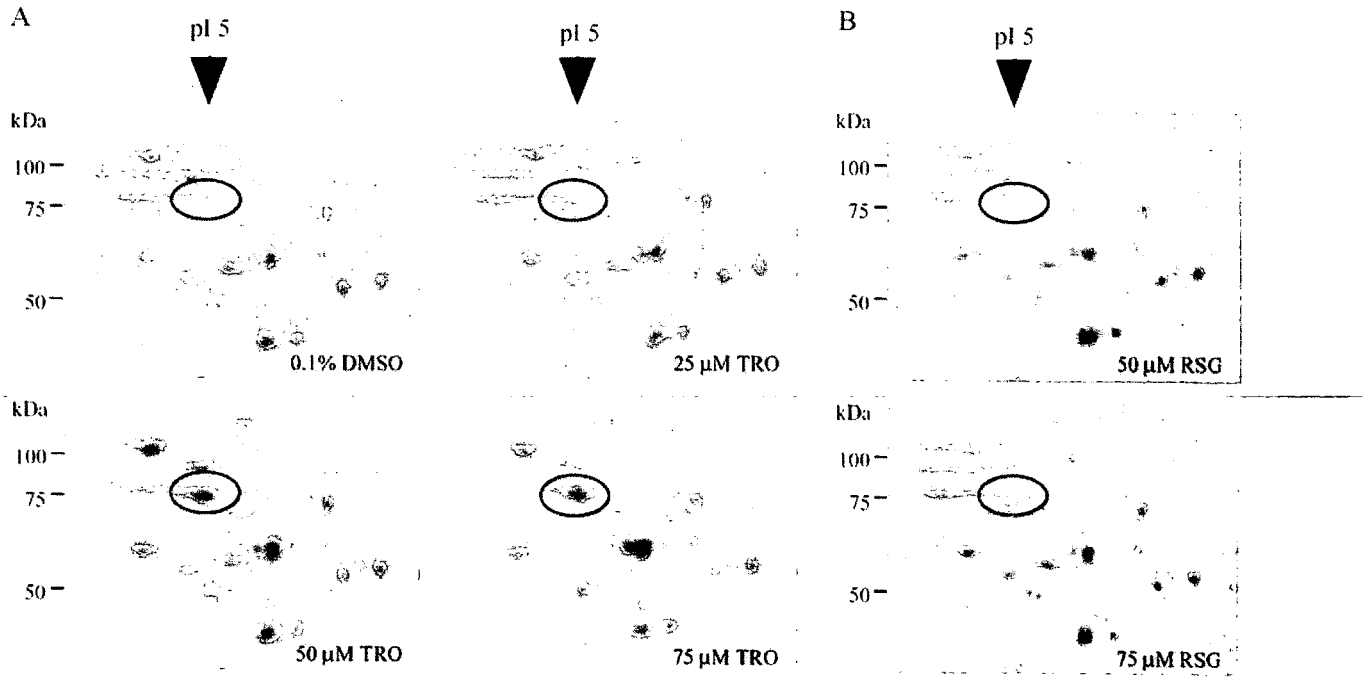

FIG. 2. Protein expression profiles of 2-D gels from CBB staining. HepG2 cells were incubated with 0.1% DMSO (control) or the indicated concentration of TRO or RSG for 48 h. The cell lysates were separated by 2-DE and stained with CBB. The oval frames mark the proteins of interest, which were increased in a concentration-dependent manner by TRO treatment.

A BiP

gi|6470150; Total score: 1341
BiP protein [Homo sapiens]
Nominal mass (Mr): 71002
Calculated pI: 5.23

```
  1 MEEDKKEDVG TVVGIDLGTT YSCVGVFKNG RVEIIANDQG NRITPSYVAF
 51 TPEGERLIGD AAKNQLTSNP ENTVFDAKRL IGRTWNDPSV QQDIKFLPFK
101 VVEKKTKPYI QVDIGGGQTK TFAPEEISAM VLTKMKETAE AYLGKKVTHA
151 VVTVPAYFND AQRQATKDAG TIAGLNVMRI INEPTAAAIA YGLDKREGEK
201 NILVFDLGGG TFDVSLLTID NGVFEVVATN GDTHLGGEDF DQRVMEHFID
251 LYKKKTGKDV RKDNRAVQKL RREVEKAKRA LSSQHQARIE LYKKKTGKDV
301 SETLTRAKFE ELNMDLFRST MKPVQKVLED SDLKKSDIDE IVLVGGSTRI
351 PKIQQLVKEF FNGKEPSRGI NPDEAVAYGA AVQAGVLSGD QDTGDLVLLD
401 VCPLTLGIET VGGVMTKLIP RNTVVPTKKS QIFSTASDNQ PTVTIKVYEG
451 ERPLTKDNHL LGTFDLTGIP PAPRGVPQIE VTFEIDVNGI LRVTAEDKGT
501 GNKNKITITN DQNRLTPEEI ERMVNDAEKF AEEDKKLKER IDTRNELESY
551 AYSLKNQIGD KEKLGGKLSS EDKETMEKAV EEKIEWLESH QDADIEDFKA
601 KKKELEEIVQ PIISKLYGSA GPPPTGEEDT AELHHHHHH
```

B PDIrp

gi|4758304; Total score: 294
Protein disulfide isomerase related protein
(calcium-binding protein, intestinal-related) [Homo sapiens]
Nominal mass (Mr): 73229
Calculated pI: 4.96

```
  1 MRPRKAPLLL LLLGLVQLLA VAGAEGPDED SSNRENAIED EEEEEEDDD
 51 EEEDDLEVKE ENGVLVLNDA NFDNFVADKD TVLLEFYAPW CGHCKQFAPE
101 YEKIANILKD KDPPIPVAKI DATSASVLAS RFDVSGYPTI KILKKGQAVD
151 YEGSRTQEEI VAKVREVSQP DWTPPEVTL VLTKENFDEV VNDADIILVE
201 FYAPWCGHCK KLAPEYEKAA KELSKRSPPI PLAKVDATAE TDLAKRFDVS
251 GYPTLKIFRK GRPYDYNGPR EKYGIVDYMI EQSGPPSKEI LTLKQVQEFL
301 KDGDDVIIIG VFKGESDPAY QQYQDAANNL REDYKFHHTF STEIAKFLKV
351 SQGQLVVMQP EKFQSKYEPR SHMMDVQGST QDSAIKDFVL KYALPLVGHR
401 KVSNDAKRYT RRPLVVVYYS VDPSFDYRAA TQFWRSKVLE VAKDFPEYTF
451 AIADEEDYAG EVKDLGLSES GEDVNAAILD ESGKKFAMEP EEFDSDTLRE
501 FVTAFKKGKL KPVIKSQPVP KNNKGPVKVV VGKTFDSIVM DPKKDVLIEF
551 YAPWCGHCKQ LEPVYNSLAK KYKGQKGLVI AKMDATANDV PSDRYKVEGF
601 PTIYFAPSGD KKNPVKFEGG DRDLEHLSKF IEEHATKLSR TKEEL
```

FIG. 3. Amino acid sequences analyzed from the 2-D gel spot. The protein spot of interest was excised from the CBB stained gel of the sample treated with 75 μM TRO and subjected to amino acid sequence analyses as described in Materials and Methods. The 'Bold Underlined' sequences denote peptides which matched with both BiP (A) and PDIrp (B).

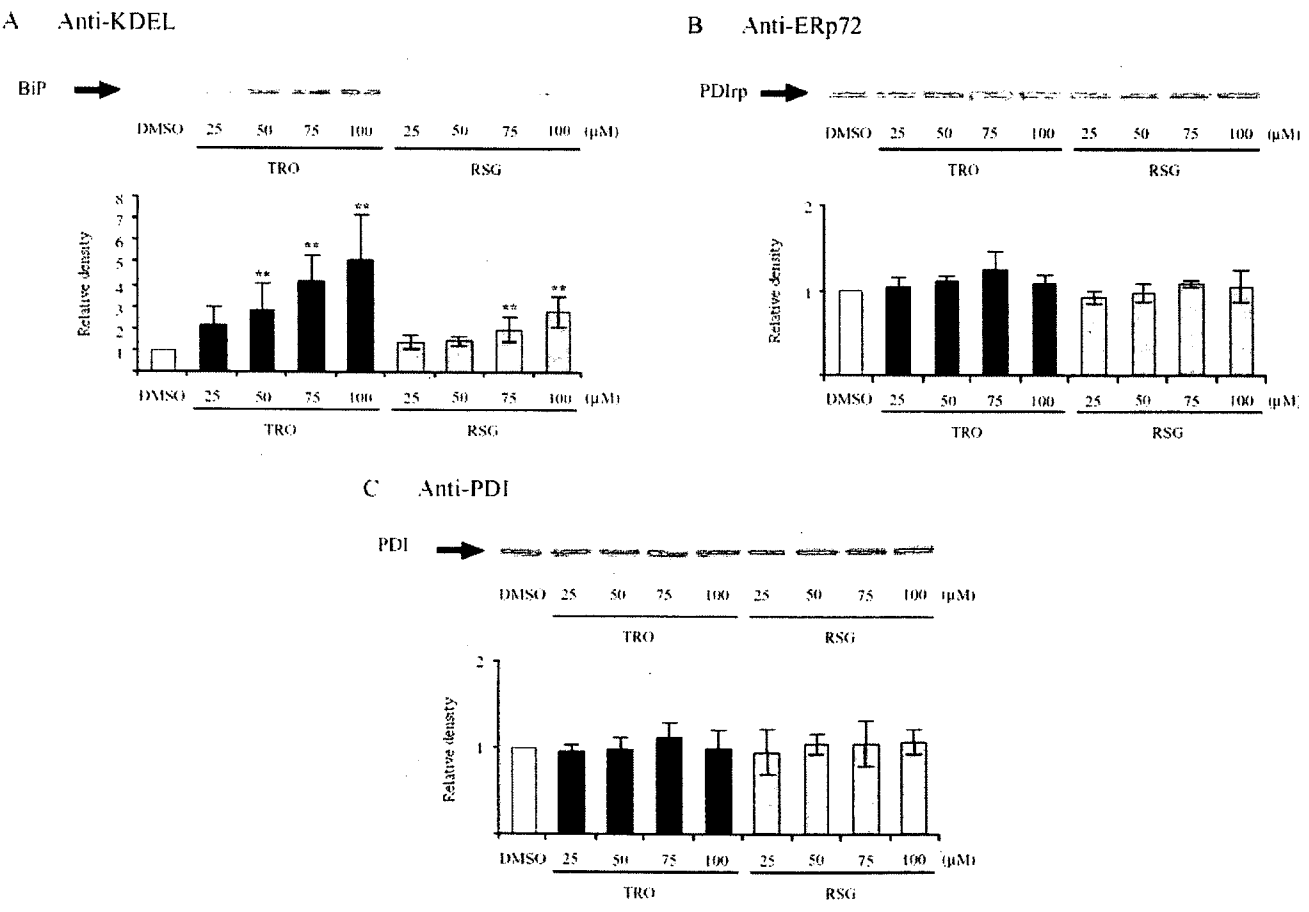

FIG. 4. Western blot analyses. HepG2 cells were incubated with 0.1% DMSO (control) or the indicated concentrations of TRO or RSG for 48 h. The cell lysates were subjected to Western blot analysis with mouse anti-KDEL (A), rabbit anti-ERp72 (B), and rabbit anti-PDI (C) antibodies for BiP, PDIrp, and PDI proteins, respectively. Two additional studies yielded equivalent results. The expressions of BiP, PDIrp, and PDI proteins were measured using a densitometer. The data represent the mean ± SD of three independent experiments. $^{**}p < 0.01$ compared with the control.

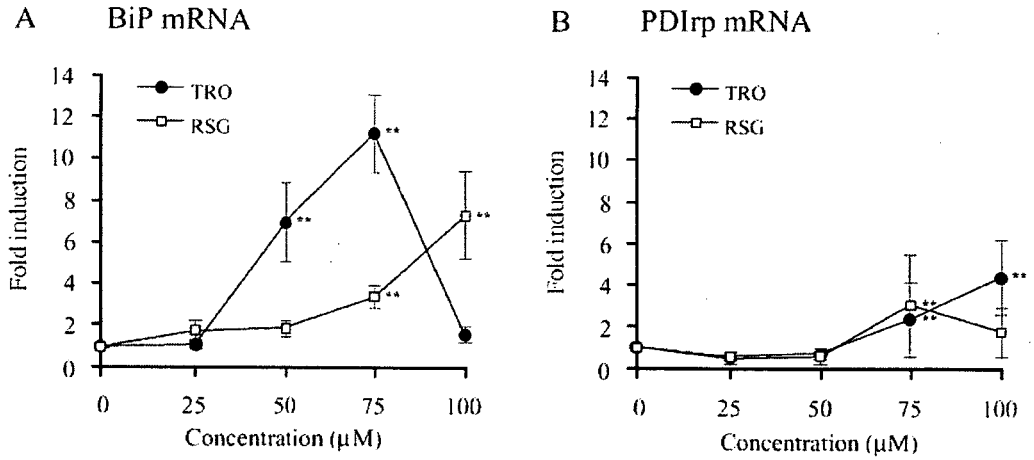

FIG. 5. Changes of BiP and PDIrp mRNA expression by TZDs in HepG2 cells. HepG2 cells were incubated with 0.1% DMSO (control) or the indicated concentrations of TRO or RSG for 48 h. The cDNA were prepared for real-time PCR. Sense and antisense primers of BiP (5′-TGCTTGATGTATGTCCCCTTA-3′ and 5′-CCTTGTCTTCAGCTGTCACT-3′) and PDIrp (5′-AATACCAGGATGCCGCTAAC-3′ and 5′-GCAAAGGTGTACTCAGGGAA-3′) were used. The relative BiP and PDIrp expression values were normalized with the GAPDH values of the same samples. The data represent the mean ± SD of three independent experiments. $^{**}p < 0.01$ compared with the control.

effects, an RNA interference technique was carried out for knockdown BiP expression. Because of the difficulty in transfecting siRNA into HepG2 cells, human hepatoma HLE cells were used instead. In our previous report, TRO possessed toxic effects on HLE cells as well as HepG2 cells, but with somewhat higher sensitivity (Yamamoto *et al.*, 2001). The BiP mRNA expression in HLE cells treated with TRO and RSG showed a similar pattern to that in HepG2 cells (data not shown). Compared to mock-transfected cells, BiP expression with DMSO treatment (control) was diminished by 50 and 100 nM of siRNA by about 30 and 17%, respectively. Furthermore, when additionally treated with 75 μM of TRO, the BiP mRNA was dramatically suppressed from 16-fold to 1.7- and 1.6-fold, respectively (Fig. 6A). Similarly, in siRNA-transfected cells treated with 100 μM of RSG, the BiP mRNA was suppressed from 2.5-fold to 0.6- and 1.0-fold, respectively (Fig. 6A). The BiP protein expression was also investigated in HLE cells after transfection with 50 nM BiP siRNA and subsequent treatment with TRO and RSG at concentrations of 75 and 100 μM, respectively. Figure 6B shows the inhibition of BiP protein production compared to the mock-transfected control under both control (DMSO) and treatment conditions assessed by Western blot analyses.

Cell Viability Changes by Troglitazone Treatment in BiP-Suppressed Cells

BiP inhibition by siRNA was clearly demonstrated, especially in the presence of TRO and RSG, to be superior to that of the mock-transfected control. Accordingly, HLE cells were then investigated in terms of the phenotypic changes. The ATP-based luminescent assay was used to measure the cell viability. In the DMSO-treated control there was a dose-dependent decrease in cell viability by BiP siRNA transfection (Fig. 7A), whereas there were no significant changes by lamin A siRNA, a negative control of siRNA transfection (Fig. 7B). Interestingly, 50 μM TRO treatments caused a significant decrease in cell viability with 10 nM of BiP siRNA ($p < 0.05$) and a marked decreased ($p < 0.01$) at the high concentration of 25 to 100 nM of BiP siRNA compared to the DMSO-treated control (Fig.7A). The 75 μM TRO treatment demonstrated significant toxic effects ($p < 0.01$) in all BiP siRNA-transfected concentrations including the mock-transfected cells (transfected control). RSG at the concentration of 75 and 100 μM showed comparable results with the DMSO with both BiP siRNA and lamin A siRNA transfection (Figs. 7A and 7B).

DISCUSSION

The toxicological potential of TRO compared to that of another TZD agent, RSG, was investigated in a human hepatoma cell line, HepG2. In this study, TRO treatment showed concentration-dependent cytotoxicity with an approximate IC_{50} of 40 μM, whereas only a slight decrease in cell viability was found with RSG treatment (Fig. 1A). These results were consistent with the previous reports, which additionally revealed that the lethal effects are exemplified by apoptosis (Bae *et al.*, 2003; Bae and Song, 2003; Yamamoto *et al.*, 2001). In our findings, the toxic effects of TRO in HepG2 cells were also exhibited in a time-dependent manner (Fig. 1B) and were significantly observed from 24 h of exposure. Although RSG showed a significant decrease in cell viability from 48 h to 60 h ($p < 0.05$), cell viabilities were more than 80% of the control

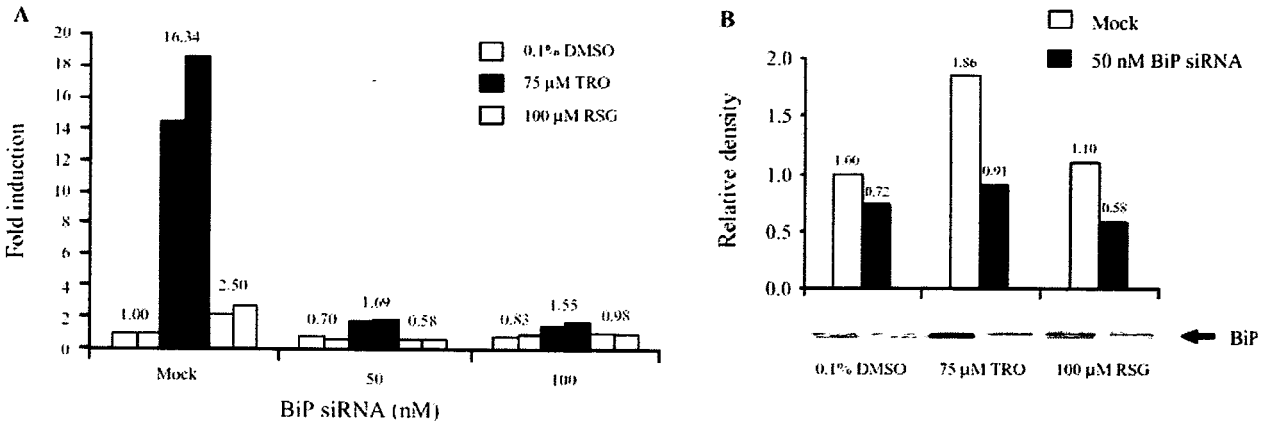

FIG. 6. Inhibitory effects of BiP siRNA on the BiP mRNA and protein expression. (A) HLE cells were transfected with 50 or 100 nM of BiP siRNA for 24 h. TRO or RSG was added to the transfection medium to make a final concentration of 75 μM or 100 μM, respectively. DMSO (0.1%) treatment was used as a control. The cells were further incubated for 24 h. The cDNA was prepared for real-time PCR. Sense and antisense primers of BiP (5′-TGCT-TGATGTATGTCCCCTTA-3′ and 5′-CCTTGTCTTCAGCTGTCACT-3′) were used. The relative BiP expression values were normalized with the GAPDH values of the same samples. (B) HLE cells were transfected with 50 nM of BiP siRNA for 24 h. TRO or RSG was added to the transfection medium to make a final concentration of 75 μM or 100 μM, respectively. DMSO (0.1%) treatment was used as a control. The cells were further incubated for 24 h. The cell lysates were prepared and subjected to Western blot analysis with mouse anti-KDEL antibody for detecting BiP protein. The expression of BiP protein was measured using a densitometer. The data represent the average value of duplicate determinations.

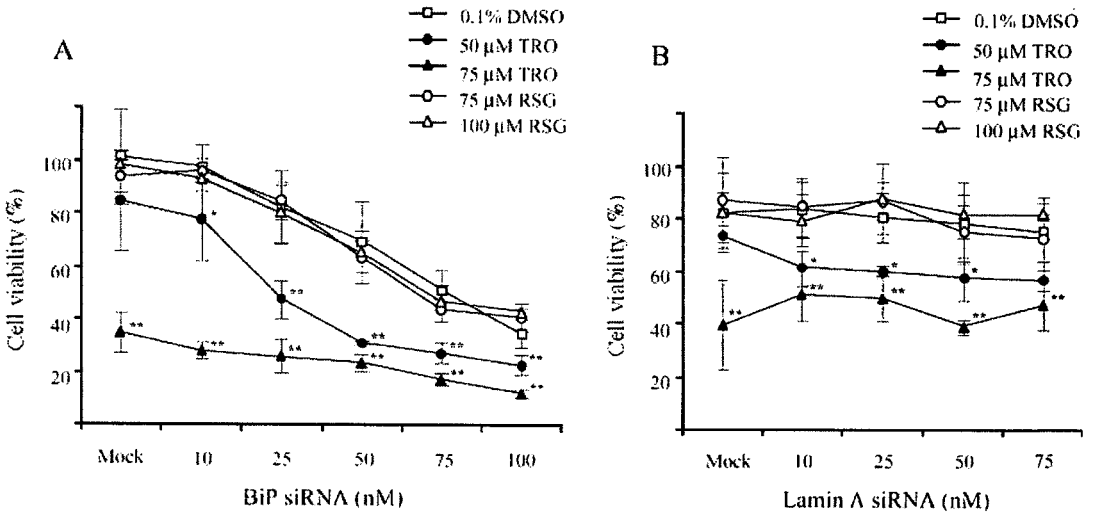

FIG. 7. Effects of BiP inhibition on cell viability. HLE cells were transfected with various concentrations of BiP siRNA (A) or lamin A siRNA as the negative control (B) for 24 h. TRO or RSG was added to the transfection medium to make a final concentration as indicated. DMSO (0.1%) treatment was used as a control. The cells were further incubated for 24 h. Cell viabilities were determined by ATP-based luminescent assay as described in Materials and Methods. The cell viability values were calculated with cell viability of the non-treated cells as 100% (neither transfection reagent nor TZDs). The data represent the mean ± SD of at least three independent experiments. $*p < 0.05$, $**p < 0.01$ compared with the control.

(Fig. 1B). The crystal violet assay in our protocol could not detect the time-dependent cytotoxicity, because the cells were not adherent before 24 h after seeding. We also confirmed with the trypan blue exclusion assay in a time-course experiment from 4 to 60 h. The percent cell viabilities were comparable to those detected with crystal violet, and significant lethal effects were observed from 12 to 60 h by 50 μM TRO exposure (data not shown). TRO has been reported to be metabolized to three main metabolites: sulfate-conjugated, glucuronide-conjugated, and quinone-type (TRO quinone) metabolites (Izumi *et al.*, 1997a,b; Kawai *et al.*, 1998). TRO, but not RSG, contains a 6-hydroxy-5,7,8-trimethylchromane moiety, which undergoes metabolic activation by hepatic cytochrome P450 enzymes, CYP2C8 and CYP 3A4, to generate TRO quinone (Tettey *et al.*, 2001; Yamazaki *et al.*, 1999). Based on the general involvement of quinones in cytotoxicity, TRO quinone has been reported to have a possible association with TRO-induced hepatotoxicity (Neuschwander-Tetri *et al.*, 1998). Previously, we

found a major epoxide of the quinone metabolite of TRO in HepG2 cells (Yamamoto *et al.*, 2002). However, the toxicity possessed by either TRO quinone or the epoxide of TRO quinone is relatively lower than that of the parent compound (Tettey *et al.*, 2001; Yamamoto *et al.*, 2001, 2002). Thus, the hepatotoxic effects were more likely due to TRO or other unknown metabolites.

Since the remarkable cytotoxicity of TRO has been established, we used 2-DE to investigate the protein expression profiles of HepG2 cells treated with various concentrations of TRO or RSG. On 2-D gels, more than ten different spots according to the treatments were revealed (small part shown in Fig. 2). We focused on a spot of interest at an approximate MW of 75 kDa and isoelectric point of 5, which showed distinct dose-dependency and TRO-specific changes with the greatest expression. The protein spot was highly matched with BiP and also, to a lesser extent, PDIrp (Fig. 3). These proteins are recognized as chaperone proteins that reside in the ER (Gething and Sambrook, 1992).

BiP, known as a 78 kDa glucose-regulated protein (Grp78), is related to the highly conserved 70 kDa heat shock protein (hsp70) family (Munro and Pelham, 1986). Apart from its response to heat, BiP is also the best-characterized chaperone and is abundantly and constitutively expressed in the ER of all eukaryotic cells (Gething and Sambrook, 1992; Haas, 1994). This protein is responsible for normal cellular functions such as assisting protein folding, assembly, and disassembly for maintenance, as well as the degradation of untenable proteins. BiP production can be induced by various perturbations of ER functions such as the expression of mutant proteins or protein subunits, reductive stress, ER Ca^{2+} depletion, and the inhibition of asparagine (N)-linked glycosylation (Gething and Sambrook, 1992; Haas, 1994; Kaufman, 1999, Lee, 2001). In our study, TRO treatment elicited a dose-dependent overexpression of BiP protein, as confirmed by Western blot analyses (Fig. 4A). BiP mRNA was also induced by treatment with 50 and 75 μM of TRO (Fig. 5A). At 100 μM TRO treatment, which resulted in about 15% cell viability, the highest induction of BiP protein was observed, but not the mRNA. Gülow *et al.* (2002) reported that under ER stress conditions, BiP expression is tightly controlled post-transcriptionally, allowing the cells to produce more proteins which are independent from the transcription level. As shown in Figure 6B, we confirmed that, with the inhibition of BiP mRNA expression before TRO or RSG treatment, the induction of BiP protein could not be achieved. Thus, the effects of 100 μM TRO treatment could be in part explained by the high translation efficiency of BiP protein in HepG2 cells. In our observation, RSG treated-HepG2 cells also induced BiP expression but at a low level, which would account for its lower toxicity compared to TRO.

Protein disulfide isomerase-related protein (herein referred to as PDIrp), or 72 kDa endoplasmic reticulum protein (ERp72), is also a resident chaperone in the ER which shares amino acid sequences with ERp59 (PDI) and holds three copies of the thioredoxin active unit as well as PDI activity *in vitro* (Gething and Sambrook, 1992; Mazzarella *et al.*, 1990). In normal cells, PDIrp is expressed constitutively at low levels and is induced by the same treatments that affect BiP expression (Huang *et al.*, 1989). We found PDIrp close to the BiP spot. However, unlike BiP, PDIrp protein was expressed equally in all treatments (Fig. 4B). Given the similar characteristics between PDIrp and PDI (Mazzarella *et al.*, 1990), we also investigated the PDI protein level in the same set of treated samples using its specific antibody. Indeed, the PDI protein expression showed comparable results (Fig. 4C) to PDIrp. Although a small induction of PDIrp mRNA was observed at the high doses of 75 and 100 μM, neither treatment lead to the overproduction of the protein. These present data suggest that the damage caused by TRO treatment was unlikely related to the increased PDI proficiency.

In order to confirm the prominent regulation of BiP by TRO-induced cytotoxicity, the RNA interference method was applied to HLE, another human hepatoma cell line. In the condition of siRNA transfection with TRO treatment, BiP expression was suppressed by about 90% compared to the corresponding mock-transfected cells (Fig.6A). This finding was reflected by the phenotypic change in cell viability. TRO caused changes in the permeability and structure of mitochondria as well as a depletion of ATP, which were correlated with the decrease of cell viability (Tirmenstein *et al.*, 2002). With a small amount of cells, the luminescent assay was considered to be sufficiently sensitive to detect the relative ATP (Fig. 1C) and showed parallel results with the cell viability in Figure 1A. Thus, to observe the phenotypic changes caused by the TRO-induced suppression of BiP, ATP produced by metabolically active cells was used as a biomarker in this study. Comparing the results in Figures 7A and 7B, we found that the inhibition of BiP appeared to promote cell death even in the absence of TRO. This supports the crucial function of BiP in normal cellular processes (Gething and Sambrook, 1992; Haas, 1994; Kaufman, 1999). Doses of 50 and 75 μM TRO as well as 75 and 100 μM RSG, which caused the high levels of BiP mRNA expression, were used. Interestingly, in the presence of 50 μM TRO, the inhibition of BiP expression rendered cells more susceptible to the lethality, as demonstrated by a gradual increase in significant cell toxicity along with the increase in the concentration of BiP siRNA (Fig. 7A). Supporting this finding, a related study reported that inhibition of BiP synthesis sensitizes cells to oxidative stress (Liu *et al.*, 1998). These phenotypic changes in cell viability suggested the crucial role of BiP overexpression in the effects of TRO exposure.

It is well known that ER is a major cellular storage site of Ca^{2+} in the cell, and ER chaperones also play important roles in Ca^{2+} accumulation and release. Both BiP and PDIrp are Ca^{2+}-binding proteins (Lee, 2001). Any disturbance in the ER homeostasis causes a release of Ca^{2+}, which in turn blocks ER protein processing, resulting in the accumulation of incompletely folded proteins, and activates the transcription of ER chaperone genes including *BiP* (Liu *et al.*, 1998; Lodish and Kong, 1990).

In previous reports, TRO but not RSG exhibited antiproliferative effects on cultured cells via a depletion of Ca^{2+} from the storage site that results in the inhibition of translation initiation (Fan *et al.*, 2004; Palakurthi *et al.*, 2001). Together with our results, it might be postulated that TRO acts as a chemical signal that causes the release of Ca^{2+} from the ER, and that BiP expression is one of the cellular responses induced by TRO toxicity. In addition, the effects of TRO on the activation of JNK pathway (Bae and Song, 2003), disturbance of mitochondria function, and depletion of ATP (Tirmenstein *et al.*, 2002) may also converge in the ER stress response (Breckenridge *et al.*, 2003).

In conclusion, the possibility was raised in the present study that the ER is one of the targets involved in TRO hepatotoxicity. TRO may serve as a stress signal to the ER, which in turn causes the overproduction of BiP in response to cytotoxicity. Supporting this view, the inhibition of BiP at the post-transcriptional level sensitized the cells to lethality.

ACKNOWLEDGMENTS

This work was supported in part by a grant from the Ministry of Education, Science, Sports, and Culture of Japan, and by Research on Advanced Medical Technology and Welfare of Japan. We thank Mr. Brent Bell for reading the manuscript.

REFERENCES

Bae, M. A., Rhee, H., and Song, B. J. (2003). Troglitazone but not rosiglitazone induces G1 cell cycle arrest and apoptosis in human and rat hepatoma cell lines. *Toxicol. Lett.* **139,** 67–75.

Bae, M. A., and Song, B. J. (2003). Critical role of c-Jun N-terminal protein kinase activation in troglitazone-induced apoptosis of human HepG2 hepatoma cells. *Mol. Pharmacol.* **63,** 401–408.

Breckenridge, D. G., Germain, M., Mathai, J. P., Nguyen, M., and Shore, G. C. (2003). Regulation of apoptosis by endoplasmic reticulum pathways. *Oncogene* **22,** 8608–8618.

Fan, Y. H., Chen, H., Natarajan, A., Guo, Y., Harbinski, F., Iyasere, J., Christ, W., Aktas, H., and Halperin, J. A. (2004). Structure-activity requirements for the antiproliferative effect of troglitazone derivatives mediated by depletion of intracellular calcium. *Bio. Med. Chem. Lett.* **14,** 2547–2550.

Freid, J., Everitt, D., and Boscia, J. (2000). Rosiglitazone and hepatic failure. *Ann. Intern. Med.* **132,** 164.

Fujiwara, T., Yoshioka, S., Yoshioka, T., Ushiyama, I., and Horikoshi, H. (1988). Characterization of new oral antidiabetic agent CS-045, Studies in *KK* and *ob/ob* mice and Zucker fatty rats. *Diabetes* **37,** 1549–1558.

Gething, M. J., and Sambrook, J. (1992). Protein folding in the cell. *Nature* **355,** 33–45.

Gitlin, N., Julie, N. L., Spurr, C. L., Lim, K. N., and Juarbe, H. M. (1998). Two cases of severe clinical and histologic hepatotoxicity associated with troglitazone. *Ann. Intern. Med.* **129,** 36–38.

Gülow, K., Bienert, D., and Haas, I. G. (2002). BiP is feed-back regulated by control of protein translation efficiency. *J. Cell Sci.* **115,** 2443–2452.

Haas, I. G. (1994). BiP (GRP78), an essential hsp70 resident protein in the endoplasmic reticulum. *Experientia* **50,** 1012–1020.

Huang, S. H., Tomich, J. M., Wu, H., Jong, A., and Holcenberg, J. (1989). Human deoxycystidine kinase, sequence of cDNA clones and analysis of expression in cell lines with and without enzyme activity. *J. Biol. Chem.* **264,** 14762–14768. Erratum in: *J. Biol. Chem.* **266,** 5353.

Isley, W. L., and Oki, J. C. (2000). Rosiglitazone and liver failure. *Ann. Intern. Med.* **133,** 393.

Izumi, T., Enomoto, S., Hoshiyama, K., Sasahara, K., and Sugiyama, Y. (1997a). Pharmacokinetic stereoselectivity of troglitazone, an antidiabetic agent, in the KK mouse. *Biopharm. Drug Dispos.* **18,** 305–324.

Izumi, T., Hoshiyama, K., Enomoto, S., Sasahara, K., and Sugiyama, Y. (1997b). Pharmacokinetics of troglitazone, an antidiabetic agent: Prediction of *in vivo* stereoselective sulfation and glucuronidation from *in vitro* data. *J. Pharmacol. Exp. Ther.* **280,** 1392–1400.

Kaufman, R. J. (1999). Stress signaling from the lumen of the endoplasmic reticulum: Coordination of gene transcriptional and translational control. *Genes Dev.* **13,** 1211–1233.

Kawai, K., Odaka, T., Tsurata, F., Tokui, T., Ikeda, T., and Nakamura, K. (1998). Stereoselective metabolism of new oral anti-diabetic agent troglitazon estereoisomers in liver. *Xenobio. Metab. Dispos.* **13,** 362–368.

Lebovitz, H. E., Kreider, M., and Freed, M. I. (2002). Evaluation of liver function in type 2 diabetic patients during clinical trials. *Diabetes Care* **25,** 815–821.

Lee, A. S. (2001). The glucose-regulated proteins: Stress induction and clinical applications. *Trends Biochem. Sci.* **26,** 504–510.

Lehmann, J. M., Moore, L. B., Smith-Oliver, T. A., Wilkison, W. O., Willson, T. M., and Kliewer, S. A. (1995). An antidiabetic thiazolidinedione is a high affinity ligand for peroxisome-activated receptor γ (PPARγ). *J. Biol. Chem.* **270,** 12953–12956.

Liu, H., Miller, E., van de Water, B., and Stevens, J. L. (1998). Endoplasmic reticulum stress proteins block oxidant-induced Ca^{2+} increases and cell death. *J. Biol. Chem.* **273,** 12858–12862.

Lodish, H. F., and Kong, N. (1990). Perturbation of cellular calcium blocks exit of secretory proteins from the rough endoplamic reticulum. *J. Biol. Chem.* **265,** 10893–10899.

Mazzarella, R. A., Srinivasan, M., Haugejorden, S. M., and Green, M. (1990). ERp72, an abundant luminal endoplasmic reticulum protein, contains three copies of the active site sequences of protein disulfide isomerase. *J. Biol. Chem.* **265,** 1094–1101.

Munro, S., and Pelham, H. R. B. (1986). An Hsp70-like protein in the ER: Identity with the 78 kD glucose-regulated protein and immunoglobulin heavy chain binding protein. *Cell* **46,** 291–300.

Nakagawa, T., Sawada, M., Gonzalez, F. J., Yokoi, T., and Kamataki, T. (1996). Stable expression of human CYP2E1 in Chinese hamster cells: High sensitivity to *N,N*-dimethylnitrosamine in cytotoxicity testing. *Mutat. Res.* **360,** 181–186.

Neuschwander-Tetri, B. A., Isley, W. L., Oki, J. C., Ramrakhiani, S., Quiason, S. G., Phillips, N. J., and Brunt, E. M. (1998). Troglitazone-induced hepatic failure leading to liver transplantation. *Ann. Intern. Med.* **129,** 38–41.

Nolan, J. J., Ludvik, B., Beerdsen, P., Joyce, M., and Olefsky, J. (1994). Improvement in glucose tolerance and insulin resistance in obese subjects treated with troglitazone. *N. Engl. J. Med.* **331,** 1188–1193.

Palakurthi, S. S., Aktas, H., Grubissich, L. M., Mortensen, R. M., and Halperin, J. A. (2001). Anticancer effects of thaiazolidinediones are independent of peroxisome proliferators-activated receptor γ and mediated by inhibition of translation initiation. *Cancer Res.* **61,** 6213–6218.

Rothwell, C., McGuire, E. J., Altrogge, D. M., Masuda, H., and de la Iglesia, F. A. (2002). Chronic toxicity in monkeys with the thiazolidinedione antidiabetic agent troglitazone. *J. Toxicol. Sci.* **27,** 35–47.

Shibuya, A., Watanabe, M., Fujita, Y., Saigenji, K., Kuwao, S., Takahashi, H., and Takeuchi, H. (1998). An autopsy case of troglitazone-induced fulminant hepatitis. *Diabetes Care* **21,** 2140–2143.

Tettey, J. N., Maggs, J. L., Rapeport, W. G., Pirmohamed, M., and Park, B. K. (2001). Enzyme induction dependent bioactivation of troglitazone and troglitazone quinone *in vivo*. *Chem. Res. Toxicol.* **14,** 965–974.

Tirmenstein, M. A., Hu, C. X., Gales, T. L., Maleeff, B. E., Narayanan, P. K., Kurali, E., Hart, T. K., Thomas, H. C., and Schwartz, L. W. (2002). Effects of troglitazone on HepG2 viability and mitochondrial function. *Toxicol. Sci.* **69,** 131–138.

Watanabe, T., Ohashi, Y., Yasuda, M., Takaoka, M., Furukawa, T., Yamoto, T., Sanbuissho, A., and Manabe, S. (1999). Was it possible to predict liver dysfunction caused by troglitazone during the nonclinical safety studies? *Iyakuhin Kenkyu* **30,** 537–546.

Watkins, P. B., and Whitcomb, R. W. (1998). Hepatic dysfunction associated with troglitazone. *N. Engl. J. Med.* **338,** 916–917.

Yamamoto, Y., Nakajima, M., Yamazaki, H., and Yokoi, T. (2001). Cytotoxicity and apoptosis produced by troglitazone in human hepatoma cells. *Life Sci.* **70,** 471–482.

Yamamoto, Y., Yamazaki, H., Ikeda, T., Watanabe, T., Iwabuchi, H., Nakajima, M., and Yokoi, T. (2002). Formation of a quinone epoxide metabolite of troglitazone with cytotoxic to HepG2 cells. *Drug Metab. Dispos.* **30,** 155–160.

Yamazaki, H., Shibata, A., Suzuki, M., Nakajima, M., Shimada N., Guengerich, F. P., and Yokoi, T. (1999). Oxidation of troglitazone to a quinone-type metabolite catalyzed by cytochrome P-450 2C8 and P-450 3A4 in human liver microsomes. *Drug Metab. Dispos.* **27,** 1260–1266.

Xenobiotica, June 2005; 35(6): 549–560

Taylor & Francis
Taylor & Francis Group

Inhibitory effects of psychotropic drugs on mexiletine metabolism in human liver microsomes: Prediction of *in vivo* drug interactions

Y. HARA[1,2], M. NAKAJIMA[1], K.-I. MIYAMOTO[2], & T. YOKOI[1]

[1]*Drug Metabolism and Toxicology, Division of Pharmaceutical Sciences, Graduate School of Medical Science, Kanazawa University, Kanazawa, Japan, and* [2]*Kanazawa University Hospital, Kanazawa, Japan*

(Received 17 February 2005)

Abstract

Mexiletine, an anti-arrhythmic agent, is used for the control of ventricular arrhythmias and for neuropathic pain from cancer or diabetes mellitus. It is sometimes used together with psychotropic drugs in patients with depression, schizophrenia or sleep disorder. It is metabolized mainly by cytochrome P450 (CYP) 2D6 and, to a minor extent, by CYP1A2. To predict possible drug interactions between mexiletine and psychotropic drugs, the inhibitory effects of 14 psychotropic drugs (phenytoin, carbamazepine, fluvoxamine, paroxetine, fluoxetine, citalopram, sertraline, imipramine, desipramine, haloperidol, thioridazine, olanzapine, etizolam, and quazepam) on mexiletine metabolism in human liver microsomes were determined. Fluoxetine ($K_i = 0.6 \pm 0.1\,\mu M$), sertraline ($K_i = 7.6 \pm 0.8\,\mu M$) and desipramine ($K_i = 3.2 \pm 0.5\,\mu M$) competitively inhibited the mexiletine *p*-hydroxylation in human liver microsomes. Thioridazine ($K_{is} = 0.5 \pm 0.2\,\mu M$; $K_{ii} = 3.6 \pm 1.6\,\mu M$) and paroxetine ($K_{is} = 1.7 \pm 0.7\,\mu M$; $K_{ii} = 3.6 \pm 0.9\,\mu M$) exhibited a mixed-type inhibition (competitive and non-competitive) toward mexiletine *p*-hydroxylation in human liver microsomes. The changes of the *in vivo* clearance of mexiletine by the psychotropic drugs were predicted by $1 + (I/K_i)$ using the *in vitro* K_i and unbound inhibitor concentrations in liver. The values were calculated as 2.4 for paroxetine, 5.5 for fluoxetine, 1.1 for sertraline, 2.8 for desipramine and 2.2 for thioridazine. In addition, paroxetine exhibited a mechanism-based inactivation with $K_i = 0.7\,\mu M$ and $K_{inact} = 0.15\,min^{-1}$. The present study predicted the possibility of drug interactions between mexiletine and paroxetine, fluoxetine, desipramine, and thioridazine in clinical use.

Keywords: *Mexiletine, cytochrome P450, psychotropic drug, inhibition, inactivation*

Correspondence: T. Yokoi, Drug Metabolism and Toxicology, Division of Pharmaceutical Sciences, Graduate School of Medical Science, Kanazawa University, Kakuma-machi, Kanazawa 920-1192, Japan. Tel/Fax: 81-76-234-4407. E-mail: TYOKOI@kenroku.kanazawa-u.ac.jp

ISSN 0049-8254 print/ISSN 1366-5928 online
DOI: 10.1080/00498250500158134

Introduction

Mexiletine is a class 1B anti-arrhythmic agent used for the control of ventricular arrhythmias and its anti-arrhythmic activity and toxicity are highly correlated with the plasma concentration of mexiletine and its therapeutic index is narrow (Campbell et al. 1978). Mexiletine is also used for the treatment of neuropathic pain from cancer and diabetes mellitus. In addition, 10–30% of cancer patients have psychological distress (Kugaya et al. 2000; Okamura et al. 2000; Akechi et al. 2001; Uchitomi et al. 2003). In the diabetic population, 24% of patients have depression (Goldney et al. 2004). Thus, mexiletine is sometimes used together with psychotropic drugs in patients with schizophrenia, depression and sleep disorders. There is abundant literature on the pharmacokinetic interactions between psychotropic drugs (Gram et al. 1974; Cooper et al. 1979; Lane 1996; Kurtz et al. 1997; Preskorn 1998). Almost all of those are due to the inhibition of cytochrome P450 (CYP) 2D6, which is a major metabolic enzyme for such psychotropic drugs. Mexiletine is metabolized to pharmacologically inactive *p*-hydroxymexiletine and 2-hydroxymexiletine mainly by CYP2D6 and, to a minor extent, by CYP1A2 (Nakajima et al. 1998). Therefore, the possibility of an interaction between mexiletine and psychotropic drugs should be considered. To predict the *in vivo* drug interactions, the present study investigated the inhibitory effects of psychotropic drugs on mexiletine metabolism in human liver microsomes. We selected 14 psychotropic drugs (phenytoin, carbamazepine, fluvoxamine, paroxetine, fluoxetine, citalopram, sertraline, imipramine, desipramine, haloperidol, thioridazine, olanzapine, quazepam and etizolam) (Figure 1) that may possibly be co-administered with mexiletine.

Materials and methods

Chemicals and reagents

Mexiletine [1-(2,6-dimethylphenoxy)-2-aminopropane] hydrochloride and *p*-hydroxymexiletine [1-(2,6-dimethyl-4-hydroxyphenoxy)-2-aminopropane] hydrochloride were kindly provided by Nippon Boehringer Ingelheim (Hyogo, Japan). Phenytoin, carbamazepine, imipramine hydrochloride, desipramine hydrochloride and haloperidol were purchased from Wako Chemicals (Tokyo, Japan). 5-Methoxyindol 3-acetic acid and fluoxetine were purchased from Sigma-Aldrich (St Louis, MO, USA). Fluvoxamine maleate was from Tocris Cookson (Ballwin, MO, USA). Paroxetine hydrochloride, citalopram, sertraline and olanzapine were purchased from Toronto Research Chemicals (Toronto, Canada). Thioridazine hydrochloride was kindly provided by Novartis Pharma AG (Basel, Switzerland). Quazepam and etizolam were kindly supplied by Mitsubishi Pharma (Osaka, Japan). $NADP^+$, glucose 6-phosphate, and glucose 6-phosphate dehydrogenase were from Oriental Yeast (Tokyo, Japan). Pooled human liver microsomes were obtained from BD Gentest (Woburn, MA, USA). All other chemicals were of the highest grade commercially available.

Mexiletine hydroxylase activity

Mexiletine hydroxylase activity in human liver microsomes was determined as reported (Nakajima et al. 1998). A typical incubation mixture (0.2 ml total volume) contained 100 mM potassium phosphate buffer (pH 7.4), an NADPH-generating system (0.5 mM $NADP^+$, 5 mM glucose 6-phosphate, 5 mM $MgCl_2$, 1 U ml^{-1} glucose 6-phosphate dehydrogenase), 0.5 mg ml^{-1} microsomal protein and mexiletine as a substrate. Each psychotropic drug, which was dissolved in methanol, was added as an inhibitor so that the

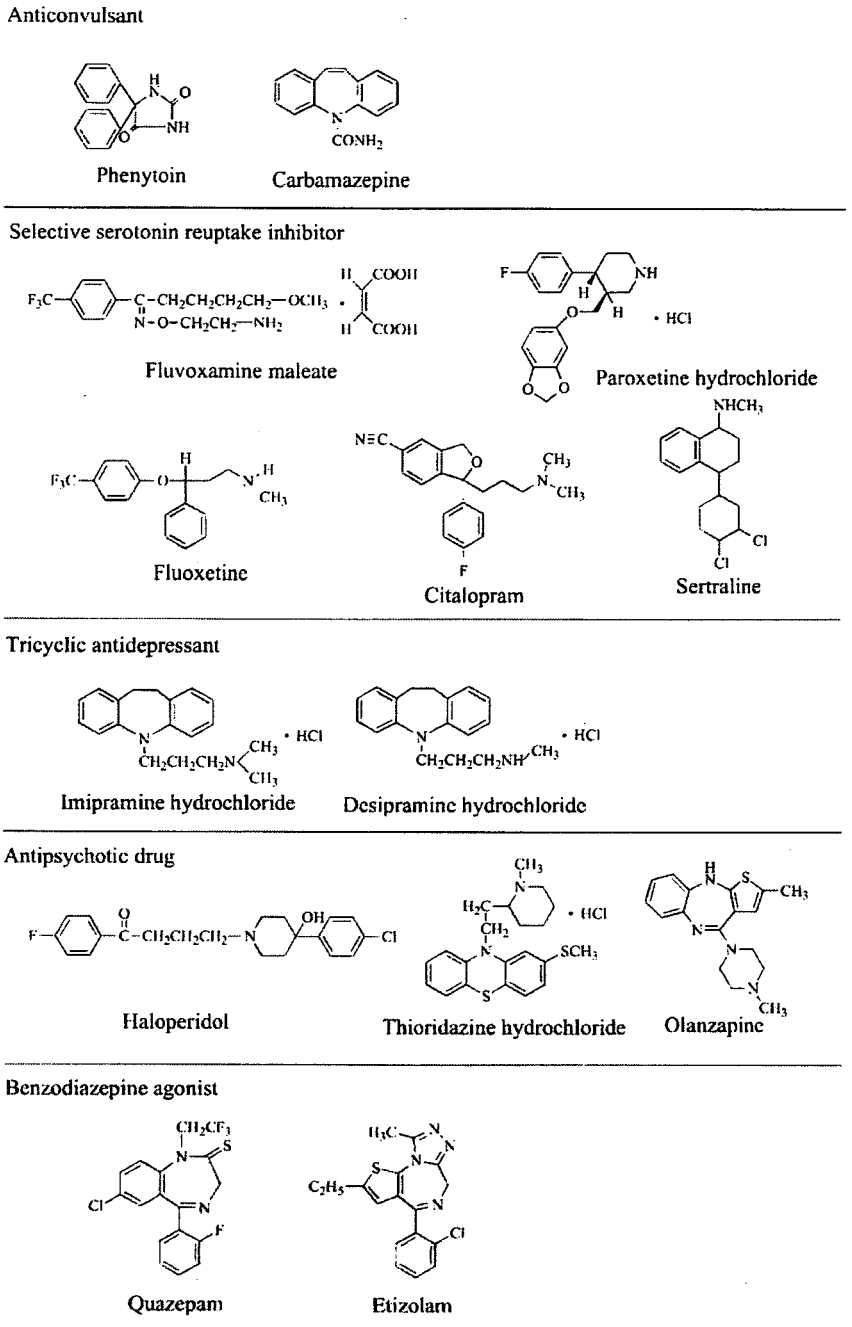

Figure 1. Structures of the psychotropic drugs used.

final concentration of solvent in the incubation mixture was <1%. The reaction was initiated by the addition of the NADPH-generating system following a 2-min pre-incubation at 37°C. The reaction was terminated by the addition of 0.1 ml ice-cold methanol, and 5-methoxyindole 3-acetic acid (10 ng) was added as an internal standard. After the removal

of protein by centrifugation at 10 000*g* for 5 min, a 100-μl portion of the supernatant was subjected to HPLC. Chromatography was performed using an L-2130 pump, an L-2480 FL detector, an L-2200 autosampler, a D-2500 integrator and an L-2300 column oven (Hitachi, Tokyo, Japan). The flow rate was 1.0 ml min^{-1} and the column temperature was 35°C. The hydroxylated metabolites were detected fluorometrically (excitation 270 nm, emission 312 nm) with a noise-base clean Uni-3 (Union, Gunma, Japan). The analytical column was a Capcell Pak C_{18} UG120 (4.6 × 250 mm; 5 μm) column (Shiseido, Tokyo, Japan) and the mobile phase was 10% acetonitrile containing 10 mM potassium dihydrogen phosphate (pH 4.5). The retention times of *p*-hydroxymexiletine, 2-hydroxymexiletine, 5-methoxyindole 3-acetic acid and mexiletine were 8.5, 11.0, 31.0 and 50.0 min, respectively. The quantification of the metabolite was performed by comparing the HPLC peak heights with that of authentic standard with reference to the internal standard.

Mechanism-based inactivation of human CYPs by paroxetine

Human liver microsomes were pre-incubated at 37°C for 10, 20 and 30 min with various concentrations of paroxetine (0.13, 0.25 and 0.50 μM final concentrations) in the presence of an NADPH-generating system. After pre-incubation, the mexiletine hydroxylase activities at a 20 μM substrate concentration were measured according to the method described above. Kinetic parameters of the inactivation process, k_{inact} and K_i, were calculated as described (Nakajima et al. 1999).

Data analyses

Lineweaver–Burk plots were used for the determination of the type of inhibition (Segel 1993), and Dixon plots were used as a secondary method. Kinetic parameters were determined by non-linear regression analysis using a computer program (K-cat, BioMetallics, Princeton, NJ, USA). All data were analysed using the average of duplicate determinations.

Prediction of interaction at clinical doses from in vitro *data*

If an enzyme reaction is inhibited competitively by other drugs, the velocity (V) is expressed as follows:

$$V = V_{max} \frac{S}{\{K_m(1 + [I/K_i]) + S\}}$$

where I and S are the concentration of the inhibitor and substrate, respectively. When the substrate concentration is much lower than K_m ($K_m \gg S$), the change in the intrinsic clearance (CL_{int}) is expressed as follows:

$$\frac{CL_{int}(+\text{inhibitor})}{CL_{int}(-\text{inhibitor})} = \frac{1}{(1 + [I_u/K_i])}$$

where I_u is the unbound concentration of the inhibitor and K_i is the inhibition constant. When we discuss drug–drug interactions via inhibition of CYP, it is important that the concentration of the inhibitor refers to the concentration of the drug at CYP. It is difficult to know the actual concentrations of drugs at the active site of CYP. In the present study, the changes of CL_{int} caused by psychotropic drugs were predicted using the maximum